Int. J. Econ. Environ. Geol. Vol. 8 (4)33-40, 2017
Journal home page: www.econ-environ-geol.org

Open Access
ISSN: 2223-957X

X-ray Diffraction Study of Aquamarine from Shigar Deposits, Skardu Valley, Northwest Pakistan

Manzoor Ahmad Badar[1], Safdar Hussain[1], Shanawer Niaz[2]*, Saif Ur Rehman[3]

[1]Department of Physics, University of Sargodha, Sargodha, Pakistan
[2]Department of Physics, University of Sargodha, Sub-campus Bhakkar, Pakistan
[3]Department of Earth Sciences, University of Sargodha, Sargodha, Pakistan

*Email: shanawersi@gmail.com

Received: *29 June, 2017* ***Accepted:*** *18 December, 2017*

Abstract: Samples of aquamarine collected from pegmatite rocks in Shigar mines, Skardu valley were investigated by powder X-ray diffraction method. Qualitative phase analyses of the samples showed the presence of aquamarine as major phase with quartz, talc and magnesite as minor phases. Lattice parameters were determined by employing CuK_α radiations in step-scan mode using a computer program 'Powder'. The lattice parameters of the Shigar specimens (with CuK_α wavelength = 0.15418 nm) are a = 9.214 ± 0.002 (Å), c = 9.202 ± 0.002 (Å) compared to NBS (National Bureau of Standards) beryl data a = 9.215 Å, c =9.192Å. The deviations in the unit cell dimensions (especially the increase in a) of the samples are attributed to the presence of additional components (Cr, Fe, Na and Mg) detected by X-ray fluorescence method.

Keywords: Shigar valley, aquamarine, beryl, powder diffraction, lattice parameters.

Introduction

Naturally occurring gemstone beryl is a common accessory mineral and almost a perfect specimen; therefore, it has been thoroughly investigated by X-ray diffraction. The green variety of beryl is called 'emerald' while its bluish type is called 'aquamarine'. As an important raw material, strategic metal beryllium is recovered from non-gem quality beryl (Webster, 1955). The low dislocation density of beryl may be a helpful point for constructing good monochromators for synchrotron soft X-rays (Wong, et al., 1982). Beryl contains a large number of trace elements particularly alkali metals depending upon the type of host rock.

Beryl is chemically a silicate of beryllium and aluminium ($Be_3Al_2Si_6O_{18}$) with hexagonal space group, P6/mcc and 2 numbers of formula units per unit cell (Morosin, 1972). Bragg and West (1926) determined the structure of beryl. They showed that the true axial ratio (c/a) is twice the ratio previously adopted by crystallographers. In the unit cell, Al site is bounded by six oxygen atoms in octahedral coordination, whereas Si and Be both by four oxygen atoms in tetrahedral coordination. The SiO_4 tetrahedra form six-member rings parallel to (001) plane and results in large open channels parallel to z-axis. In these positions, they link the oxygen atoms of Si_6O_{18} rings and the whole structure is like a honeycomb with open channels. Most of the substitutions occur at the Y site. The rings have their centres on hexad axes and are stacked on one another. Two of the oxygen atoms in each SiO_4 group are shared by other SiO_4 group and the rings lie on the (001) planes with the silicon atoms sharing oxygen atoms. Aluminium and beryllium atoms lie between them, each Al linked to an octahedral group of six oxygen atoms and each Be atom bounded by four oxygen atoms on a distorted tetrahedron. Belov and Mateeva (1950) refined and confirmed the structure of beryl suggested by Bragg and West (1926). Ginzburg (1955) found from their data that the channels of beryl contain alkali metal and water molecules. Detailed work of Wood and Nassau (1968) with their spectroscopic absorption data, led to the recognition of two types of water in beryl. They demonstrated that the Type I water is oriented in the hollow channels with its diad axis perpendicular to the z-axis of beryl. The Type II water molecule is rotated by 90° by the action of a nearby alkali ion on the molecular dipole and lies with its symmetry axis parallel to z-axis. Two sites known in the hexagonal channels are marked as 2a at (0, 0, 0.25) and 2b at (0, 0, 0) positions (Artioli, et al., 1993). They recommended that, in alkali and water-rich beryl varieties the larger alkali atoms (Cs, Rb, K) and water molecules occupy the 2a site, and Na atoms occupy the smaller 2b position. In alkali and water poor beryl variety, both Na atoms and water molecules occur at the 2a site with 2b site empty.

The presence of appreciable alkali ions, particularly the large Cs^+ ion causes an increase in the cell parameters, with the 'c' dimension increasing more than the 'a' dimension (Sosedko, 1957). Radcliffe and Campbell (1966) suggested that substitution of larger ion R^+ within the structure increases 'c' dimension and substitution in the channels expands 'a' dimension. Filho, et al., (1973) analysed a series of 28 Na-K beryl samples from Brazil and obtained unit cell parameters as a = 9.210 to 9.245Å and c = 9.190 to 9.220Å. Badar, et al., (2017) investigated green emerald from Mingora and Charbagh's Carbonate-Talc rocks in Swat Valley with powder XRD and

Copyright © SEGMITE

XRF methods. Qualitative phase analyses showed emerald as major phase with quartz, talc and magnesite as minor phases. The impurities elements Fe, Cr, Na and Mg detected by XRF indicate the structural substitutions which probably changed the lattice parameters.

The aim of the present study on Shigar aquamarine samples from Skardu valley is two-fold: (i) to find the lattice parameters and (ii) to assess the effect of impurities on the lattice parameters. An X-ray powder diffractometer equipped with scintillation counter for qualitative analysis and X-ray fluorescence spectrometer for elemental analysis were employed. A computer program 'Powder' (Taktai and Schaqnulis, 1972) calculated the lattice parameters.

Specimen geology

Beryl group of minerals (emerald and aquamarine) are mostly found in vugs or cavities in granites and granite pegmatite. It occurs as massive form in pegmatites and occasionally in metamorphic rocks. Emerald is found either along sheers in the carbonate talc rocks or in quartz veins. According to Davies (1962), better crystals of aquamarine are to be found in softer carbonate talc environment and in granite pegmatite due to the small size of Be ion, concentrated in the residual magmatic fluids. Many worldwide pegmatite rocks are well-known among the mineral and gemstone collectors for various gemstones like emerald (London, 1986; Vianna, et al., 2002). Gem-bearing pegmatite of northern Pakistan are famous in the world for fine quality aquamarine, topaz, garnet and tricoloured tourmaline (Kazmi, et al., 1985; Kazmi and O'donoghue, 1990). Pegmatite-hosted emeralds within Pakistan are known only from the Khaltaro deposit. Snee, et al., (1989) have reported the chemical analyses of emeralds from several Pakistani locations including Khaltaro. Sinkankas (1981) as well as Kazmi and Snee (1989) included a complete account of known beryl mineralization from numerous worldwide localities and reviewed several modes of its formation.

The major emerald deposits in Pakistan are the Mohmand and Malakand areas, the Swat Valley in the Northwestern areas, the Bajaur Agency and the Khaltaro area in the Gilgit-Baltistan. In the Mohmand area at the Gandao deposit, 40 Km NW of Peshawar, beryl variety emerald is found in quartz veins in a dolomite host (Grundmann and Giuliani, 2002). The Swat Valley is about 200 km NE of Peshawar among the leading mines spread around the NE edge of Mingora town. An inky blue beryl from Swat State is similar to one described by Schaller et al., (1962) from Arizona, USA, which was reported to contain high Cs and low Li contents (Shams, 1963). In the Swat valley, Gujarkili is the next most significant emeralds mining district (Bowersox and Anwar, 1989; Schwarz and Giuliani, 2002). The emeralds crop up mostly with fuchsite and Cr-rich tourmaline in limonitized shear zones inside talc-carbonate rocks traversed by small quartz veins (Kazmi, et al., 1986; Arif, et al., 1996). The Gemstone Corporation of Pakistan, approximately 70 km NE of Gilgit in the Northern Pakistan, discovered the Khaltaro minerals deposit, in 1985. Similarly, the deposits of bluish green to light green aquamarine are found at several localities in Shigar and Hunza valleys of northern Pakistan (Agheem, et al., 2011).

The northern and northwestern parts of Pakistan are characterized by the collage of different tectonic elements including Eurasian Plate, Kohistan-Ladakh Arc and Indian Plate from north to south, respectively, formed by the collision of Indian and Eurasian plates by sandwiching the sequence of Kohistan-Ladakh Arc (Tahirkheli et al., 1979; Bignold and Treloar, 2003; Aitchison et al., 2007). Eurasian Plate collided first with Kohistan-Ladakh Arc at 85Ma along the Northern Suture Zone followed by the initial contact of Indian Plate with aforementioned arc along the Southern Suture Zone at the terminal of Upper Cretaceous (Spencer, 1994; Searle et al., 1996, 1999; Yin, 2006).

Table 1 X-ray powder diffractometer conditions for calibration and collection of data on Shigar aquamarine in continuous and step-scan modes.

Diffractometer conditions	**Continuous-scan mode**	**Step-scan mode**
Tube voltage	35 kV	35 kV
Tube current	20 mA	20 mA
Radiation	Cu Kα	Cu Kα
Start angle for Cu, Si, (beryl)	100°	5°
Stop angle for Cu, Si, (beryl)	5°	100°
Goniometer Scanning speed	1°/min	0.5O/min
Preset time	1 sec	1 sec
Divergence slit/Anti scatter slit	1°	1°
Receiving slit	0.15 mm	0.15 mm
Detector	Scintillation counter	Scintillation counter

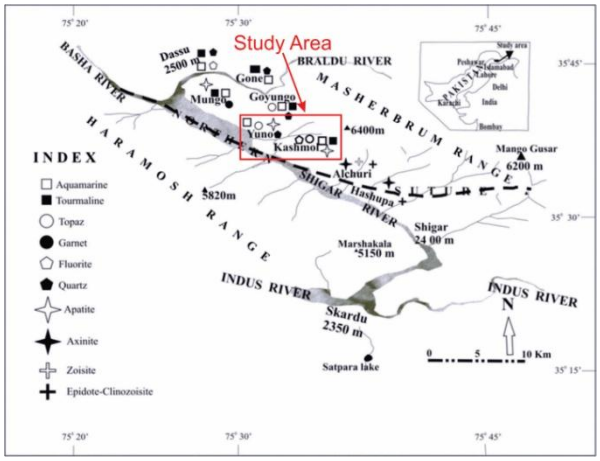

Fig. 1 Geological map of Shigar valley showing location of Kashmol and Yuno aquamarine deposit, North west Pakistan (modified after Agheem et al., 2014).

The final collision between Indian Plate and Kohistan-Ladakh Arc and closure of Neotethys was occurred at the terminal of Eocene which placed the Kohistan-Ladakh sequence over the rocks of Indian Plate along the Southern suture zone (Petterson and Treloar, 2004; Yin, 2006; Aitchison et al., 2007; Khan et al., 2009, 2012, 2013). Post collisional convergence caused the crustal shortening, regional metamorphism, folding and faulting and uplifts which emplaced the large mountain ranges in the northern part of Pakistan including Himalaya, Karakoram and Hindukush ranges (Yin, 2006; Aitchison et al., 2007).

The Shigar valley (latitude: 35° 25′ 32″ N and longitude: 75° 43′ 59″ E), located in the north of Skardu occupies the areas of Kohistan-Ladakh arc and Karakoram Range and crops out the rocks of Kohistan-Ladakh arc, Northern suture zone and Karakoram block (Fig.1modified after Agheem, et al., 2014). This is the most renowned valley of the Gilgit-Baltistan

Table 2 X-ray diffraction data for light green aquamarine from Shigar valley, Northwest Pakistan.

d-value Observed	d-value Standard	I/I_1 Observed	I/I_1 Standard	H K L
7.999	7.98	76	90	100
4.604	4.60	33	50	110, 002
4.261*	-	-	-	-
3.986	3.99	29	45	200, 102
3.343*	-	-	-	-
3.254	3.254	94	95	112
3.012	3.015	33	35	210, 202
2.864	2.867	100	100	211
2.658	2.660	3	4	300
2.520	2.523	18	30	212
2.297	2.293	7	12	220, 302
2.209	2.208	6	4	104
2.149	2.152	11	16	311
2.055	2.056	4	6	114
1.991	1.9926	13	20	312, 204
1.829	1.8308	4	8	320, 402
1.792	1.7954	9	18	321, 313
1.738	1.7397	16	20	304
1.709	1.7110	8	14	411
1.626	1.6265	10	18	412, 224
1.594	1.5953	6	8	500, 314
1.569	1.5690	6	8	215
1.531	1.5320	5	8	006
1.512	1.5138	10	16	413
1.454	1.4535	7	12	116
1.431	1.4324	8	14	510
1.366	1.3656	6	6	216
1.296	1.2977	2	<1	513, 325
1.276	1.2774	8	12	520, 602
1.264	1.2628	9	9	432
1.215	1.2170	3	2	610
1.204	1.2041	8	9	217
1.149	1.1490	3	4	700
1.138	1.1396	2	3	434
1.116	1.1173	4	7	442, 524
1.085	1.0848	1	2	336
1.074	1.0752	2	4	426, 218
1.068	1.0683	3	5	533, 435
1.048	1.0485	3	4	417
1.015	1.0157	2	3	541, 615

Table 3 XRD data (2θ, d-values and texture coefficients with lattice parameters) for green aquamarine from Shigar Skardu in continuous-scan mode with nickel filtered radiation Cuk_{α}.

HKL	2θ(degree) Observed	2θ(degree) Calculated	d-value Standard Å	d-value Observed Å	d-Value Calculated Å	HKL	Texture Coefficients
100	10.99	11.053	7.98	8.0504	8.0046	100	1.12
002	19.18	19.263	4.60	4.6073	4.6076	110	0.88
112	27.29	27.332	3.254	3.0279	3.0215	200	0.86
202	29.50	29.563	3.013	3.0156	3.0142	112	1.32
211	31.09	31.113	2.867	2.8672	2.8659	210	1.26
300	33.55	33.586	2.660	2.6601	2.6598	211	1.34
212	35.50	35.495	2.523	2.5226	2.5223	300	1.00
302	39.00	39.008	2.293	2.2977	2.3027	212	0.80
311	41.80	41.852	2.152	2.1517	2.1517	220	0.78
204	45.39	45.424	1.9926	1.9929	1.9929	311	0.92
402	49.65	49.668	1.8308	1.8308	1.8302	312	0.87
313	50.79	50.737	1.7954	1.7944	1.7947	320	0.67
304	52.48	52.475	1.7397	1.7389	1.7399	321	0.67
411	53.41	53.384	1.709	1.7096	1.7109	-	-
+A Number of weaker peaks							
Bravais lattice type	Hexagonal	Space group	P6\mcc	a (Å)	9.243±0.003	c (Å)	9.215±0.006

region of Pakistan for gem-quality mineral deposits especially for light green aquamarine with bluish tonnage. In the Shigar valley, aquamarine occurs in pegmatites and metamorphic rocks of aforementioned sequences at several localities as Kashmol, Yunno, Mungo, Goyungo, Gone and Dassu (Agheem, et al., 2011).

Materials and Methods

In present study, five samples of light green aquamarine have been collected from the pegmatites of cropped out between the Koshmal and Yunno villages of the Shigar valley. Pieces of single crystal beryl were crushed to coarse grains of 2-5 mm in size. Subsequently the pieces of aquamarine were picked by a pair of tweezers from each sample. The aquamarine pieces were then pulverized with the help of an agate mortar and passed through 325 meshes (about 55µm) for getting uniform grain size. These sieved powders were pulverized again so that the grain size now was essentially less than 10µm. The ideal sample for X-ray diffraction is the one with homogeneous grain size of less than 10µm without any preferred orientation or strain. It is to be noted that when the particle size is large, a problem may arise simply due to statistics. Only the crystal grains with their reflection planes parallel to the sample surface can add to the diffracted intensity. When the number of such reflection planes is too small to justify the supposed random division, normally an error in the reflection peak intensity occurs. This error may be as large as 5-10%. The pulverized samples were subsequently pressed gently in aluminium holders before mounting them on the diffractometer

Table 4 X-ray diffraction data (2θ, d-values and the lattice constants for green bluish aquamarine from the Shigar Valley in Step-scan mode with nickel-filtered radiation $Cuk_{\alpha 1}$.

HKL	2θ Observed	2θ Calculated	d-value Standard	d-value Observed	d-value Calculated
100	11.047	11.088	7.98	8.0090	7.9793
002	19.266	19.291	4.60	4.6069	4.6009
102	22.278	22.304	3.99	3.9904	3.9858
112	27.387	27.396	3.254	3.2565	3.2554
202	29.623	29.636	3.015	3.0156	3.0142
211	31.194	31.208	2.867	2.3672	2.8659
300	33.692	33.696	2.660	2.6601	2.6598
212	35.588	35.592	2.523	2.5226	2.5223
302	39.172	39.119	2.293	2.2977	2.3027
104	40.805	40.822	2.208	2.2113	2.2104
311	41.988	41.988	2.152	2.1517	2.1517
114	44.008	43.995	2.056	2.0575	2.0581
204	45.514	45.514	1.9926	1.9929	1.9929
402	49.804	49.822	1.3308	1.8308	1.8302
304	52.586	52.598	1.7397	1.7403	1.7399
411	53.558	53.563	1.709	1.710	1.7109
+A number of weak reflections					
Bravais Lattice type, Space group	Hexagonal, P6\mcc	a (Å)	9.214±0.001	c (Å)	9.202±0.002

for X-ray diffraction study.

Qualitative analysis of beryl single crystals was carried out on X-Ray Powder Diffractometer model: Rigaku Geigerflex D/max-IIA at Centre for Solid State Physics, University of the Punjab, Lahore. Before collection of data, the diffractometer was calibrated by running standard pure materials like Si, Cu, Ag and quartz in continuous and step-scan modes with the conditions given in Table 1. The powder X-ray diffractometer employed in the present study is equipped with a pulse height analyser, a rate meter, a recorder and a scintillation counter. The Cu target of the system was operated at a voltage of 40 kV and filament current of 25 mA. The divergence/anti-scatter slits were 1^o/min in continuous-scan and at 0.5^o/min in step-scan modes. In the continuous-scan mode, the starting and the stopping angles for beryl data collection were 100^o and 5^o respectively, while in case of step-scan mode were respectively 5^o and 100^o. The 2θ angles and intensity of each peak in the XRD pattern were calculated. The relative integrated intensity, d-spacing's and reflection planes for peaks in the pattern are given in the Table 2. First, the d-values were found with the help of XRD tables (Fang and Bloss, 1966). The maximum intensity I_{max} and full width at half maximum of every peak were found and multiplied both to calculate the integrated intensity of the peak. Each pattern was qualitatively analysed by the well-known Hanawalt method (Hanawalt, et al., 1983).

Since each crystalline specimen gives its own characteristic XRD pattern, therefore the study of x-ray diffraction patterns of unidentified phases presents a dominant mean of qualitative phase investigation. A computer program calculated the d-spacing and intensities of every sample. The powdered XRD patterns of each specimen were analysed with the data files of ICDD (International Centre for Diffraction Data) via a computer software program and identified properly. Qualitative phase analysis of the sample XRD pattern (Fig. 2) shows that all the samples contain aquamarine beryl as the major constituent with minor traces of quartz. The XRD powder data (d-values and relative intensities) of the sample are almost similar to the XRD powder data of beryl in the NBS (National Bureau of Standards) and JCPDS (Joint Committee on Powder Diffraction Standards), Card # 09-430. The Bravais lattice of this beryl variety has been reported to be hexagonal. This aquamarine beryl specimen was therefore, indexed assuming them of hexagonal symmetry. The 2θ-values in the XRD powder data obtained for determination of lattice parameters of beryl were preliminary treated as suggested in Cullity (1978). The X-ray diffractometer employed in the present study does not give a monochromatic beam of X-rays. The X-rays coming out of the Cu tube of the diffractometer are nickel filtered for eliminating K_β radiation. The filtered radiation comprises almost of Cuk_α, which is of much higher intensity (of the order of 100 or so) than the suppressed K_β radiation. However, K_α peaks of large intensity do have K_β peaks, which appear, on the lower angle side of the former peaks. The Cuk_α(λ = 1.5418Å) radiation also consists of two lines, $Cuk_{\alpha1}$(λ = 1.5406Å) and $Cuk_{\alpha2}$(λ = 1.5443Å) doublet. Both $Cuk_{\alpha1}$ and Cuk_α were used for acquiring XRD data in the step-scan mode but only Cuk_α for the continuous-scan mode.

Microstructures have geometric and crystallographic features that affect their properties. Distribution of grain size and shape constitute geometric features. Among crystallographic are the hkl orientation of the crystallites with respect to each other and the macroscopic surface of the sample. In case of preferred orientation or texture of a flat/needle like shape specimen, the crystals are not randomly orientated. The preferred orientation of different crystal grains causes large deviations between observed and calculated intensities. In a truly random distribution, the number of particles in each orientation should be identical. However, this might not be true if the particles have anisotropic shape. In case of hexagonal powder sample with same size of particles, the (0001) reflection will come from majority of particles than other reflections like (1010). Because of this preferred orientation, the (000l)-type reflections will be stronger. This means that for each theta other crystals contribute to the intensity except of higher order reflections of course. Any change of this isotropy will affect the intensity of specific diffraction peak. For non-isotropic shaped crystals like needles or plates, the fraction of the diffraction plane is smaller or bigger than expected. However, during preparation (or simply by natural occurrence) often anisotropy in crystal orientations cannot be prevented so that this so-called texture affects the finally detectable "size" of the diffracting plane as well and influence the collected intensity. Commonly, something that alters the presumed random division of particles will influence the distribution of relative intensities. In addition, some large particles, in a powder sample can change the distribution of intensities.

Preferred orientations of the reflection planes for each beryl data were calculated before utilizing the data for unit cell size determination. The texture or preferred orientation of a plane (hkl) in a polycrystalline specimen is defined as:

Here TC (hkl) is the texture coefficient of the relevant (hkl) plane, I is the intensity measured, I_o is standard intensity of the plane in JCPDS and N is the number of peaks detected in the XRD patterns. The values of TC >1 for certain planes (100, 202, 211, 300, 212) show preferred orientation. The d-values (observed and calculated), the integrated intensities and the texture coefficients for different reflection planes in continuous-scan mode, of the Shigar beryl are presented in Table 3. It is obvious from the data in Table that except a few planes, the sample overall does not exhibit preferred orientation. X-ray diffraction data (2θ, d-values and the lattice constants of respective reflections) for green aquamarine from Shigar Skardu in Step-scan mode with nickel-filtered radiation $Cuk_{\alpha1}$ is given in Table 4. To find impurities in beryl sample, elemental analysis was performed using X-ray fluorescence spectrometer Model 3064 Higaku Corporation Japan, at Pakistan Institute of Nuclear Science & Technology, Nilore, Islamabad.

$$TC\ (hkl) = \frac{I\ (hkl)/I_o\ (hkl)}{\left(\frac{1}{N}\right) \Sigma\ I(hkl)/I_o(hkl)}$$

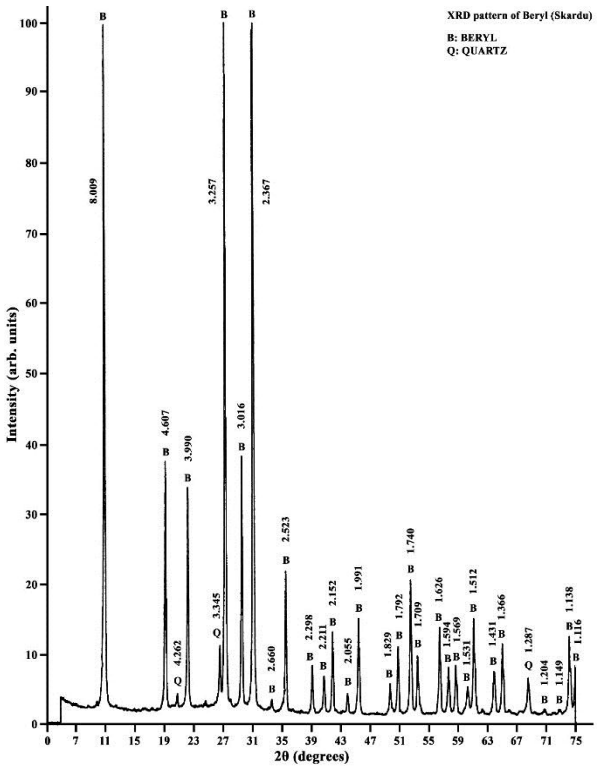

Fig.1 X-Ray powder diffractometer pattern of the sample from Koshmal, Shigar valley displaying aquamarine beryl as major phase with quartz as minor phase.

Results and Discussion

Geochemically, the Shigar valley pegmatite is granitic and categorized as simple and complex pegmatite (Hassan, 2007). The granitic pegmatite usually exhibits multifaceted mineralogy and internal arrangement (Ćerný 1982, 1991). These are classified because of different parameters such as the occurrences of gemstones, rare earth metals, presence or absence of cavities, zoning and vugs. The difference in the colour of beryl normally reveals variation in composition (Hammarstrom, 1989). Hassan (2007) described that the Shigar beryl are poor in alkalis due to low Li contents in parent pegmatite. Beryl usually contains some alkalis and in certain varieties, total alkali contents may rise to around 5 to 8%. Different studies have shown that the alkali metal contents in beryl variety from Li pegmatite are generally higher than in nonlithium pegmatite (Gallagher, 1975). In this study, XRF elemental analysis of the Shigar aquamarine indicated the presence of the elements Ca, Fe and K as impurity. Na, Li and the larger alkali ions like K and Cs are found in the beryls but Rb is less common. Folinsbee (1941) pointed out that some Na may substitute for Be, the larger ions K and Cs cannot replace Be in beryl structure. In view of wide hexagonal channels, it is probable that large alkali ions are present in channels. Schaller, et al., (1962) and Bakakin, et al., (1969) have been in agreement that the octahedral positions occupied by Al in the beryl structure may be substituted by Cr, Fe^{3+}, Fe^{2+}, Mg and Li. Alkali and alkaline earth metal ions would occupy the centres of the plane of Al and Be ions. The green colour of the beryl is associated with Cr, pink with Cs, pale yellow and inky blue with Fe. The blue colour in aquamarine is commonly due to Fe^{+2} components (Vianna, et al., 2002) and also because of variable Fe^{+3}/Fe^{+2} ratios (Figueiredo et al., 2008).

According to Sosedko (1957), the presence of appreciable amount of alkali metals (i.e. Na_2O, Li_2O and Cs_2O), particularly the large Cs^+ ion causes an increase in the unit cell parameters, with the '*c*' dimension increasing more than the '*a*' dimension. Radcliffe and Campbell (1966) suggested when the substitution of somewhat larger R^+ ion (alkali and alkaline earth metal ion Li, Na and K occurs within the structure itself, the '*c*' dimension increases. When the substituting ions are located in the channels, once a possible threshold value of about 2.5 mole % R_2O has been exceeded, the cell expands in the '*a*' dimension. Filho, et al., (1973), from a series of analysed Na-K beryl varieties from Brazil with low alkali contents obtained; '*a*' = 9.210-9.245Å and '*c*' = 9.190-9.220Å. From a statistical analysis of their data, they showed that an increase of Fe and (Fe + Mn + Mg) has a positive correlation with '*a*' but no influence on '*c*' which in turn has a close positive correlation with Li and a negative correlation with Be, there is also a positive correlation between Na and the '*a*' dimension.

Conclusion

The cell dimensions of a Royal Stone (USA) beryl reported in an NBS circular (1960) are '*a*' = 9.215Å and '*c*' = 9.192Å with an error 0.003%. The present Shigar aquamarine data (obtained with Cuk_α radiation of wave length 1.5418Å) in continuous and step-scan modes are '*a*' lattice parameter = 9.243(±0.003) Å, 9.214(±0.001) Å and '*c*' lattice parameter = 9.215(±0.006) Å, 9.202(±0.002) Å respectively. The lattice parameters are relatively close to the standard data obtained with CuK_α radiation in step-scan mode. This result was also obtained for the standard materials studied for calibrating the powder X-ray diffractometer. The impurities reported in the standard NBS beryl are 0.1-1.0% Fe, Na and Zn; 0.001-0.01% Mg, Mn, Sr and Ti. The impurity elements Fe, Ca and K detected in Shigar sample by XRF elemental analysis indicate the structural substitution that possibly changed the lattice parameters of the sample. The qualitative analysis of the Shigar beryl by X-ray diffraction patterns showed the presence of quartz as minor traces with major phase of aquamarine in beryl variety.

References

Agheem, M. H., Shah, M. T., Khan, T., Laghari, A., Dars, H. (2011). Field features and petrography used as indicators for the classification of Shigar valley pegmatites, Gilgit-Baltistan region of Pakistan. *J. himal. earth. sci.*, **44** (2), 1-7.

Agheem, M. H., Shah, M. T., Khan, T., Laghari, A., Murata, M., Arif, M., Dars, H. (2014). Shigar valley gemstones, their chemical composition and origin, Skardu, Gilgit-Baltistan, Pakistan. *Arab. J. Geosci.*, **7** (9), 3801-3814.

Aitchison, J. C., Ali, J. R., Davis, A. M. (2007). When and where did India and Asia collide? *J. Geophys. Res*., **112** (B5), 115-121.

Arif, M., Fallick, A. E., Moon, A. E. (1996). The genesis of emeralds and their host rocks from Swat, northwestern Pakistan: a stable-isotope investigation. *Miner. Depos.*, **31** (4), 255-268.

Artioli, G., Rinaldi, R., Stahl, K., Zanazzi, P. F. (1993). Structure refinements of beryl bysingle-crystal neutron and X-ray diffraction. *Am. Mineral*., **78**, 762-768.

Badar, M. A., Hussain, S., Niaz, S., Rehman, S. (2017). X-ray diffraction study of green emerald from Mingora deposits, the Swat Valley, Northwest Pakistan. *J. Himal. Earth Sci*., **50**(1), 13-24.

Bakakin, V. V., Rylov, G. M., Belov, N. V. (1969). Crystal Structure of Lithium-bearing beryl. *Dokl. Earth. Sci. Sect*., **188** (3), 136-139.

Belov, N. V., Mateeva, R. G. (1950). The determination of the structural parameters of beryl by the method of bounded projections. *Dokl. Akad. Nauk. SSSR.*, **73**, 299-302.

Bignold, S. M., Treloar, P. J. (2003). Northward subduction of the Indian plate beneath the Kohistan island arc, Pakistan Himalaya: New evidence from isotopic data. *J. Geol. Soc.*, **160**(3), 377-384.

Bowersox, G. W., Anwar, J. (1989). The Gujar Killi emerald deposit, Northwest Frontier Province, Pakistan. *Gemmology*, **25** (1), 15-24.

Bragg, W. L., West, J. (1926). The structure of beryl, $Be_3Al_2(SiO_3)_6$. In: *Proceedings of the Royal* Society *of London, Series A*, 691-714.

Ćerný, P. (1982). Anatomy and classification of granitic pegmatites. In *Granitic pegmatites in science and industry*. P. Ćerný (eds.), *Min. Soc. Can. Short. Course. Handb.*, **8**, 1-39.

Ćerný, P. (1991). Rare-element granitic pegmatites. Part 1: anatomy and internal evolution of pegmatite deposits. *Geosci Can*., **18** (2), 49-67.

Cullity, B. D. (1978). Elements of X-ray diffraction. *Edison-Wesley P Inc*. California, USA.

Davies, R. G., (1962). The nature of the upper Swat hornblendic group. *Geol. Bull. Punjab Univ*., **2**, 51-52.

Fang, J. H., Bloss, D. F. (1966). X-ray diffraction Tables. *Southern Illinois University Press*, London.

Figueiredo, M. O., Da Silva, T. P., Veiga, J. P., Gomes, C. L., De Andrade, V. (2008). The blue colouring of beryls from Licungo, Mozambique: an X-ray absorption spectroscopy study at the iron K-edge. *Mineral Mag*., **72** (1), 175-178.

Filho, H., de A. S., Sighinolfi, G. P., Galli, E. (1973). Contribution to the crystal chemistry of beryl. *Contrib. Mineral. Petrol*., **38** (4), 279-290.

Folinsbee, R. E. (1941). Optic properties of cordierite in relation to alkalies in the cordierite-beryl structure. *Am. Mineral.*, **26**, 485-500.

Gallagher, M. J. (1975). Composition of some Rhodesian lithium-beryllium pegmatites. *Trans. Geol. Soc. S. Africa*., **78** (1), 35-41.

Ginzburg, A. I. (1955). On the question of the composition of beryl. *Tr. mineralog. muzeya. akad. nauk. SSSR.*, **7**, 56-69.

Grundmann, G., Giuliani, G. (2002). Emeralds of the world. *Extra Lapis English*., **2**, 24-35.

Hammarstrom, J. M. (1989). Mineral chemistry of emeralds and some associated minerals from Pakistan and Afghanistan: an electron microprobe study. In *Emeralds of Pakistan: geology, gemology, and genesis*. A. H. Kazmi and L. W. Snee (eds.), Geological Survey of Pakistan *and Van Nostrand Reinhold Co. Inc.*, New York, 125-150.

Hanawalt, J. D., Rinn, H. W., Frevel, L. K. (1938). Chemical analysis by x-Ray Diffraction. *Ind. Eng. Chem. Anal. Ed*., **10** (9), 457-512.

Hassan, M. (2007). Mineralogy and geochemistry of the gemstones and gemstone bearing pegmatites in Shigar valley of Skardu, northern areas of Pakistan. *Unpubl. Ph. D thesis. Univ.* Peshawar, Pakistan.

Kazmi, A. H., Peters, J. J., Obodda, H. P. (1985). Gem pegmatites of the Shingus-Dusso area, Gilgit, Pakistan. *Mineral. Record*, **16 (**5), 393-411.

Kazmi, A. H., Lawrence, R. D., Anwar, J., Snee, L. W., Hussain, S. (1986). Mingora emerald deposits (Pakistan); suture-associated gem mineralization. *Econ. Geol.*, **81** (8), 2022-2028.

Kazmi, A. H., Snee, L. W. (1989). *Geology of world emerald deposits: a brief review*. Van Nostrand Reinhold publishers, The Netherlands, 165pages.

Kazmi, A. H., O'Donoghue, M. (1990). Gemstones of Pakistan: Geology and gemmology. *Gemstone Corporation of Pakistan*, Peshawar.

Khan, M. A., Rehman, S. U., Ahsan, N., Ullah, F., Ahsan, N. (2009). Geochemistry and tectonic environment of Babusar amphibolites, southeast Kohistan, Pakistan. *Geol. Bull. Punjab Univ*., **44**, 105-116.

Khan, M. A., Rehman, S. U., Ahsan, N. (2012). Geology and geochemistry of Sumal amphibolites, Kamila amphibolites unit, southeast Kohistan, Pakistan. *Int. J. Agric. Appl. Sci*., **4** (2), 99-111.

Khan, M. A., Rehman, S. U., Mehmood, K., Khan, M. A., Ahsan, N. (2013). Geochemical characterization and petrogenesis of Niat-Jal amphibolites, southeast Kohistan, Pakistan. *Iranian j. Sci. Tech.*, **37** (A2) 147-159.

London, D. (1986). Formation of tourmaline-rich gem pockets in miarolitic pegmatites. *Am. Mineral.*, **71**, 396-405.

Morosin, D. (1972). Structure and thermal expansion of beryl. *Acta. Crystallogr. B.*, **28** (6), 1899-903.

Petterson, M. G., Treloar, P. J. (2004). Volcanostratigraphy of arc volcanic sequences in the Kohistan arc, North Pakistan: Volcanism within island arc, backarc-basin, and intra-continental tectonic settings. *J. Volcanol. Geotherm. Res.*, **130** (1-2), 147-78.

Radcliffe, D., Campbell, F.A. (1966). Beryl from Birch Portage, Saskatchewan. *Can. Mineral*, **8** (4), 493-505.

Schaller, W. T., Stevens, R. E., Jahns, R. H. (1962). An unusual beryl from Arizona. *Am. Mineral.*, **47**, 672-99.

Schwarz, D., Giuliani, G. (2002). Emeralds from Asia. *Extra Lapis English*., **2**, 60-63.

Searle, M. P., Corfield, R. I., Stephenson, B. J. McCarron, J. (1996). Structure of the North Indian continental margin in the Ladakh-Zanskar Himalayas: implications for the timing of obduction of the Spontang ophiolite, India-Asia collision and deformation events in the Himalaya. *Geol. Mag*., **134** (3), 297-316.

Searle, M. P., Khan, M. A., Fraser, J. E., Gough, S. J., Jan, M. Q. (1999). The tectonic evolution of the Kohistan collision belt along the Karakorum Highway transect, north Pakistan. *Tectonics*, **18**(6), 929-49.

Spencer, D. A. (1994). Continental collision in the Northwest Himalayan Tethyan Region: In *Geology in South Asia, Proceedings, 1st South Asia Geological Congress*. R. Ahmed and A. M. Sheikh (eds.), Islamabad, Pakistan, 185pages.

Shams, F. A. (1963). An inky blue beryl from Swat State. *Geol. Bull. Punjab Univ*., **3**, 31.

Sinkankas, J. (1981). *Emerald and other beryls*, Chilton Book, Radnor, Pennsylvania.

Snee, L. W., Foord, E. E., Hill, B., Carter, S. J., (1989). Regional chemical differences among emeralds and host rocks of Pakistan and Afghanistan: implications for the origin of emerald. In *Emeralds of Pakistan: Geology, gemology, and genesis.* A. H. Kazmi and L. W. Snee, (eds.), *Van Nostrand Reinhold*, New York, 93-124.

Sosedko, T. A. (1957). The change of structure and properties of beryls with increasing amounts of alkalis. *Mem. All-union mineral. Soc.*, **86**, 495-499.

Tahirkheli, R. A. K., Mattauer, M., Proust, F., Tapponnier, P. (1979). The India-Eurasia suture zone in northern Pakistan: Synthesis and interpretation of recent data at plate scale. In *Geodynamics of Pakistan.* A. Farah and K. A. DeJong, (eds.), *Geological Survey of Pakistan*. Quetta, Pakistan, 125-130.

Taktai, L., Shaqnulis, A. J. (1972). Programme Powder, *Arizona State University*.

Vianna, R., Jordt-Evangelista, H., Costa, G., Stern, W. (2002). Characterization of beryl (aquamarine variety) from pegmatites of Minas Gerais, Brazil. *Phys. Chem. Miner*., **29** (10), 668-679.

Webster, R. (1955). The emerald. *J. Gem.*, **5** (4), 185-221.

Wong, J., Roth, W. L., Batterman, B. W., Berman, L. E., Barbee, T. (1982). Stability of some soft x-ray monochromator crystals in synchrotron radiation. *Nucl. Instr. Meth. Phys. Res.*, **195** (1-2), 133-139.

Wood, D. L., Nassau, K. (1968). The characterization of beryl by visible and infrared absorption spectroscopy. *Am. mineral.*, **53** (5-6), 777-800.

Yin, A. (2006). Cenozoic tectonic evolution of the Himalayan orogen as constrained by along-strike variation of structural geometry, exhumation history, and foreland sedimentation. *Earth-sci. rev*., **76** (1-2), 1-131.